Supplementary Materials: Effects of Alignment of Weak Interaction Sites in Molecular Shape Recognition High-Performance Liquid Chromatography

Hiroki Noguchi, Tianhang Liu, Makoto Takafuji and Hirotaka Ihara

1. Synthetic Scheme

General synthetic procedures were described in the main manuscript.

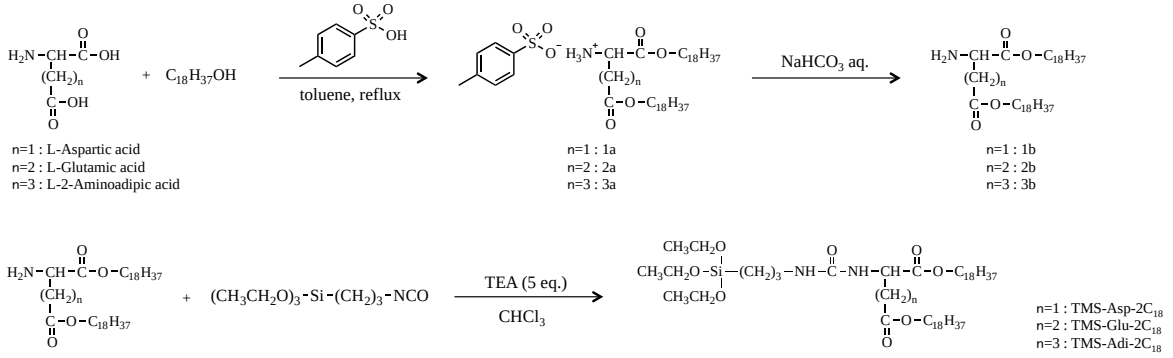

Figure S1. Synthetic scheme of amino acid derivatives for high-performance liquid chromatography (HPLC) organic phases.

2. Characterization

(1a) Yield: 72.3%; Melting point (m.p.): 88.0–90.1 °C; Fourier transform infrared (FT-IR) (KBr, cm^{-1}): 2928 (νC–H), 2853(νC–H), 1770 and 1734 (νC=O, ester), 1541 (δNH_3^+), 1473 (δC–H); ^{1}H-NMR (400 MHz, $CDCl_3$): 0.88 (6H, t, CH_3), 1.26 (60H, br, CH_2), 1.52 (4H, m, $COCH_2CH_2$), 2.35 (3H, s, $ArCH_3$), 3.19–3.01 (2H, dd, C*CH_2) (*: Chiral carbon), 3.97–4.10 (4H, m, $COCH_2$), 4.42–4.40 (1H, m, C*H), 7.12–7.14 (2H, d, ArH), 7.73–7.80 (2H, d, ArH), 8.31 (3H, s, NH_3^+); Elemental analysis calcd (%) for $C_{47}H_{87}NO_7S$: C 69.67, H 10.82, N 1.73; found C 69.25, H 10.62, N 1.75.

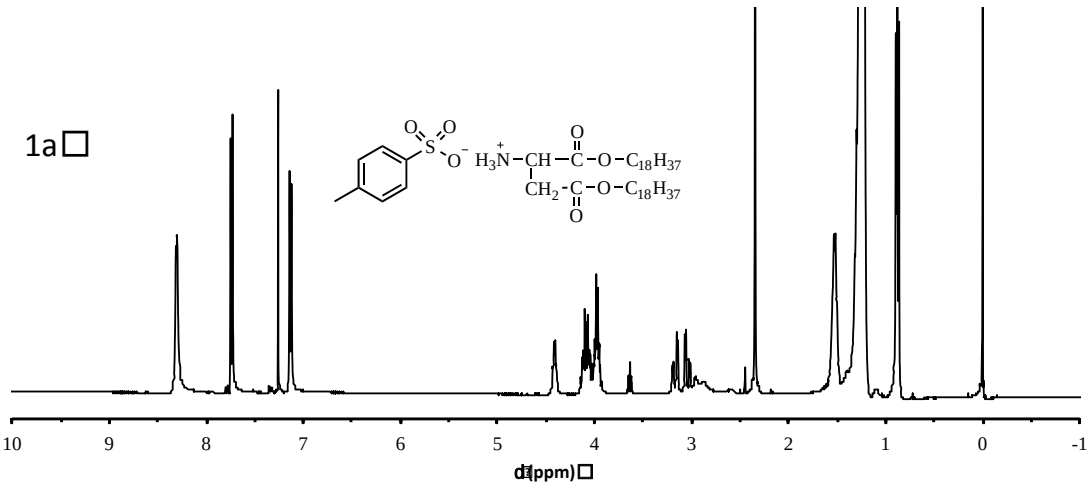

Figure S2. ^{1}H-nuclear magnetic resonance (NMR) of 1a.

(1b) Yield: 87.9%; m.p.: 62.4–64.0 °C; FT-IR (KBr, cm^{-1}): 2924 (νC–H), 2846 (νC–H), 1728 (νC=O, ester), 1473 (δC–H); ^{1}H-NMR (400 MHz, $CDCl_3$): 0.88 (6H, t, CH_3), 1.26 (60H, br, CH_2), 1.60–1.65 (4H,

m, $COCH_2CH_2$), 2.66–2.82 (2H, dd, C*CH_2), 3.79–3.82 (1H, m, C*H), 3.97–4.10 (4H, m, $COCH_2$); Elemental analysis calcd (%) for $C_{40}H_{79}NO_4$: C 75.3, H 12.48, N 2.20; found C 74.99, H 13.17, N 2.18.

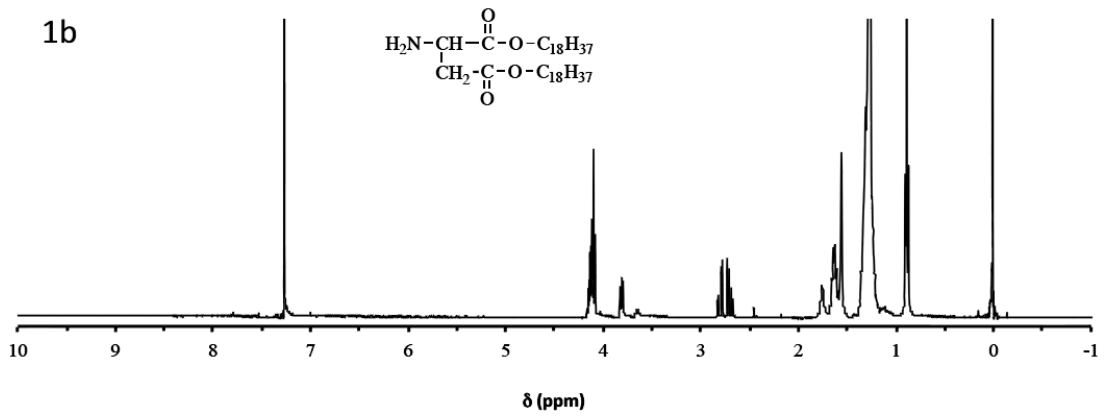

Figure S3. ^{1}H–NMR of 1b.

(1c) Yield: 90.5%; m.p.: 68.1–68.8 °C; FT-IR (KBr, cm^{-1}): 3367 and 3331 (νN–H), 2912 and 2848 (νC–H), 1750 and 1734 (νC=O, ester), 1631 (νC=O, urea), 1572 (δN–H, urea); ^{1}H-NMR (400 MHz, $CDCl_3$): 0.62–0.66 (2H, t, $SiCH_2$) 0.88 (6H, t, CH_3), 1.26 (69H, br, CH_2 and CH_3CH_2O), 1.58–1.75 (6H, m, $COCH_2CH_2$ and $SiCH_2CH_2$), 2.80–3.03 (2H, dd, C*CH_2), 3.17–3.20 (2H, q, $NHCH_2$), 3.79–3.84 (6H, q, CH_3CH_2O), 4.05 (2H, t, OCH_2), 4.12 (2H, t, OCH_2), 4.59 (1H, t, NH), 4.72–4.84 (1H, m, C*H), 5.23–5.21 (1H, d, NH); Elemental analysis calcd (%) for $C_{50}H_{100}N_2O_8Si$: C 67.82, H 11.38, N 3.16; found C 67.23, H 11.94, N 3.16.

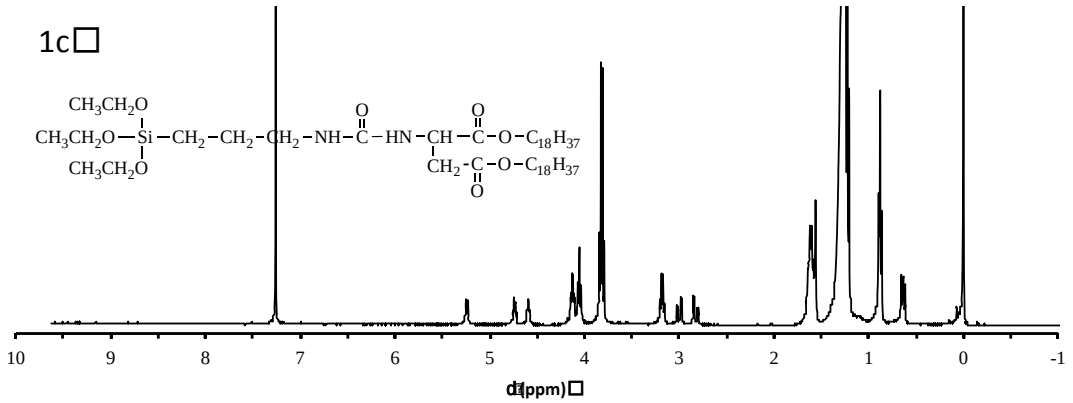

Figure S4. ^{1}H-NMR of 1c.

(2a) Yield: 78.0 %; m.p.: 70.6–71.4 °C; FT-IR (KBr, cm^{-1}): 2928 and 2049 (νC–H), 1741 and 1735 (νC=O, ester), 1541 (δNH_3^+), 1471 (δC–H); ^{1}H-NMR (400 MHz, $CDCl_3$): 0.88 (6H, t, CH_3), 1.14–1.36 (60H, br, CH_2), 1.50–1.59 (4H, m, $COCH_2CH_2$), 2.00–2.11 (2H, m, C*CH_2), 2.16–2.26 (2H, m, C*CH_2 CH_2), 3.82–4.03 (m, 4H, $COCH_2$), 7.10–7.85 (4H, d, ArH); Elemental analysis calcd (%) for $C_{48}H_{89}NO_7S$: C 69.94, H 10.88, N 1.70; found C 69.14, H 11.30, N 1.79.

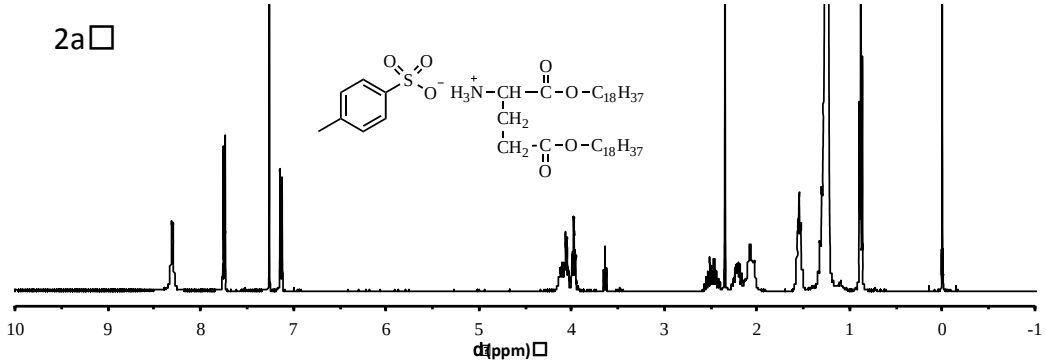

Figure S5. ^{1}H-NMR of 2a.

(2b) Yield: 80.0%; m.p.: 47.5 °C; FT-IR (KBr, cm^{-1}): 2922 (νC–H), 2843 (νC–H), 1738 (νC=O, ester), 1469 (δC–H); ^{1}H-NMR (400 MHz, $CDCl_3$): 0.88 (6H, t, CH_3), 1.14–1.36 (60H, br, CH_2), 1.59–1.64 (4H, m, $COCH_2CH_2$), 1.79–2.15 (2H, m, C*CH_2), 2.44–2.47 (2H, m, C*CH_2 CH_2), 3.44–3.48 (m, 1H, C*H), 4.05–4.12 (4H, m, OCH_2); Elemental analysis calcd (%) for $C_{41}H_{81}NO_4S$: C 75.52, H 12.52, N 2.15; found C 75.24, H 13.03, N 2.20.

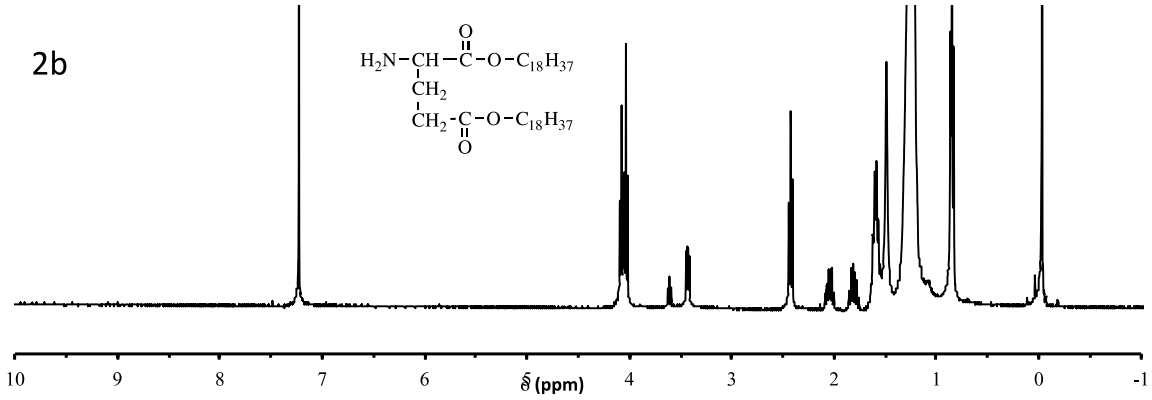

Figure S6. ^{1}H-NMR of 2b.

(2c) Yield: 79.6%; m.p.: 65.5–68.0 °C; FT-IR (KBr, cm^{-1}): 3362 and 3337 (νN–H), 2918 and 2848 (νC–H), 1745 and 1729 (νC=O, ester), 1638 (νC=O, urea), 1578 (δN–H, urea), 1473 (δC–H); ^{1}H-NMR (400 MHz, $CDCl_3$): 0.64–0.68 (2H, t, $SiCH_2$) 0.90 (6H, t, CH_3), 1.20–1.40 (69H, br, CH_2 and CH_3CH_2O), 1.62–1.66 (6H, m, $COCH_2CH_2$ and $SiOCH_2CH_3$), 1.95–2.19 (2H, m, C*CH_2), 2.37–2.46 (2H, m, C*HCH_2CH_2), 3.17–3.22 (2H, q, $NHCH_2$), 3.81–3.87 (6H, t, $SiOCH_2CH_3$), 4.05–4.13 (4H, m, OCH_2), 4.48–4.53 (1H, m, C*H), 4.61–4.62 (1H, m, NH), 4.92–4.94 (1H, d, NH); Elemental analysis calcd (%) for $C_{51}H_{102}N_2O_8Si$: C 68.10, H 11.43, N 3.11; found C 67.75, H 11.88, N 3.23.

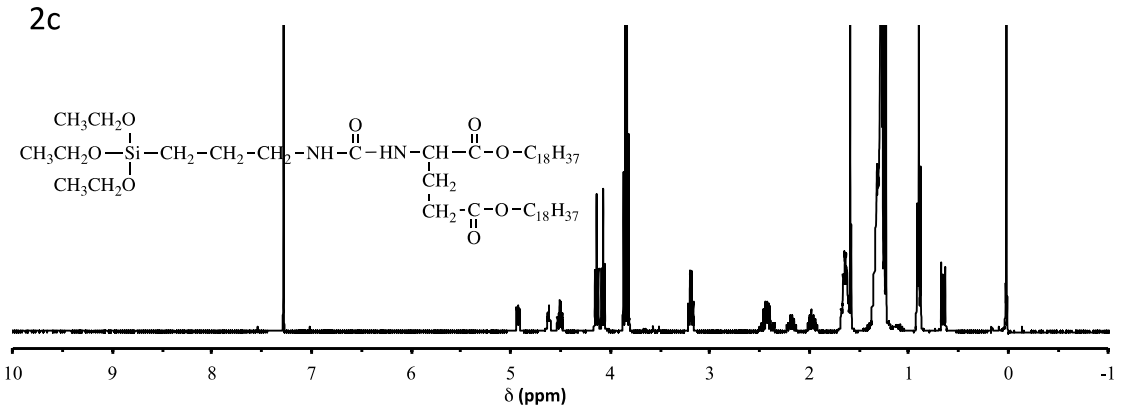

Figure S7. ^{1}H-NMR of 2c.

(3a) Yield: 75.6%; m.p.: 79.5–80.8 °C; FT-IR (KBr, cm^{-1}): 2921 and 2848 (νC–H), 1738 and 1734 (νC=O, ester), 1597 (δNH_3^+), 1463 (δC–H); ^{1}H-NMR (400 MHz, $CDCl_3$): 0.88 (6H, t, CH_3), 1.14–1.36 (60H, br, CH_2), 1.54–1.76 (6H, m, $COCH_2CH_2$, C*CH_2), 1.86–1.88 (2H, m, C*CH_2CH_2), 2.17–1.20 (m, 2H, CH_2C(=O)), 2.35 (3H, s, $ArCH_3$), 3.94–4.12 (5H, m, OCH_2, C*H) 7.13–7.15 (2H, d, ArH), 7.74–7.76 (2H, d, ArH), 8.24 (3H, s, NH_3^+); Elemental analysis calcd (%) for $C_{49}H_{91}NO_7S$: C 70.20, H 10.94, N 1.67; found C 69.83, H 11.52, N 1.67.

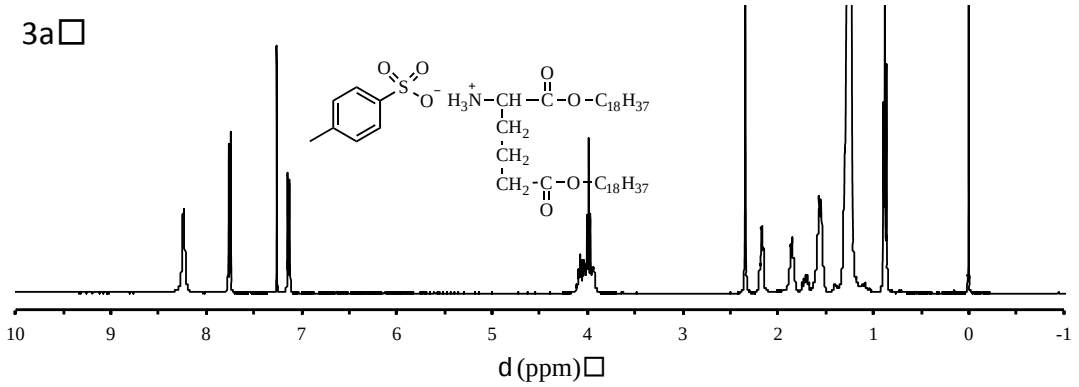

Figure S8. ^{1}H-NMR of 3a.

(3b) Yield: 91.0%; m.p.: 42.9–43.8 °C; FT-IR (KBr, cm^{-1}): 2917 and 2849 (νC–H), 1725 (νC=O, ester), 1463 (δC–H); ^{1}H-NMR (400 MHz, $CDCl_3$): 0.88 (6H, t, CH_3), 1.14–1.36 (60H, br, CH_2), 1.58–1.78 (8H, m, OCH_2CH_2, C*CH_2CH_2, C*CH_2CH_2), 2.32–2.35 (m, 2H, CH_2C(=O)), 3.42–3.45 (1H, m, C*H), 4.04–4.12 (4H, m, OCH_2); Elemental analysis calcd (%) for $C_{42}H_{83}NO_4$: C 75.73, H 12.56, N 2.10; found C 75.23, H 13.16, N 2.20.

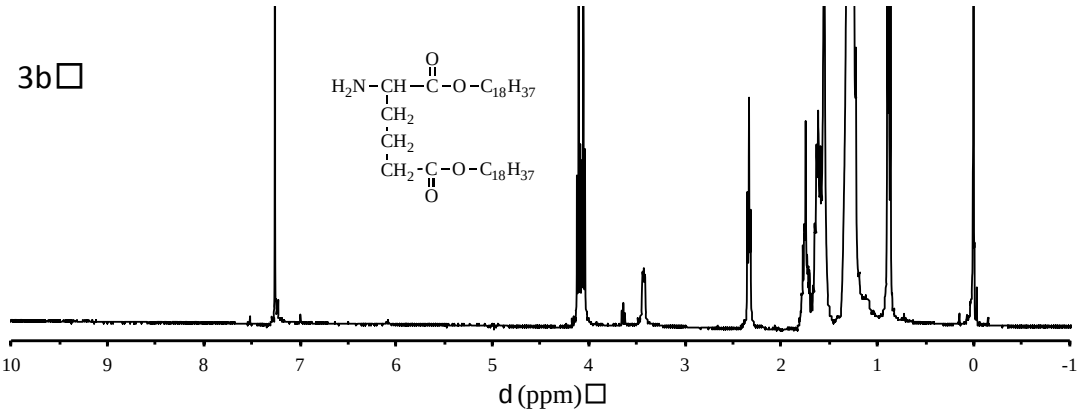

Figure S9. ^{1}H-NMR of 3b.

(3c) Yield: 83.0%; m.p. 58.8–59.7 °C; FT-IR (KBr, cm^{-1}): 3365 and 3341 (νN–H), 2916 and 2849 (νC–H), 1734 (νC=O, ester), 1630 (νC=O, urea), 1567 (δN–H, urea); ^{1}H-NMR (400 MHz, $CDCl_3$): 0.64–0.68 (2H, t, $SiCH_2$) 0.88 (6H, t, CH_3), 1.20–1.40 (69H, br, CH_2 and CH_3CH_2O), 1.59–1.67 (8H, m, C*CH_2, C*H_2CH_2, $COCH_2CH_2$ and $SiOCH_2CH_3$), 2.32–2.33 (2H, m, CH_2C(=O)), 3.15–3.20 (2H, q, $NHCH_2$), 3.79–3.84 (9H, q, $SiOCH_2CH_3$), 4.02–4.12 (4H, m, OCH_2), 4.46–4.53 (2H, m, C*H, NH), 4.80–4.82 (1H, d, NH); Elemental analysis calcd (%) for $C_{52}H_{104}N_2O_8Si$: C 68.37, H 11.48, N 3.07; found C 67.96, H 11.88, N 3.07.

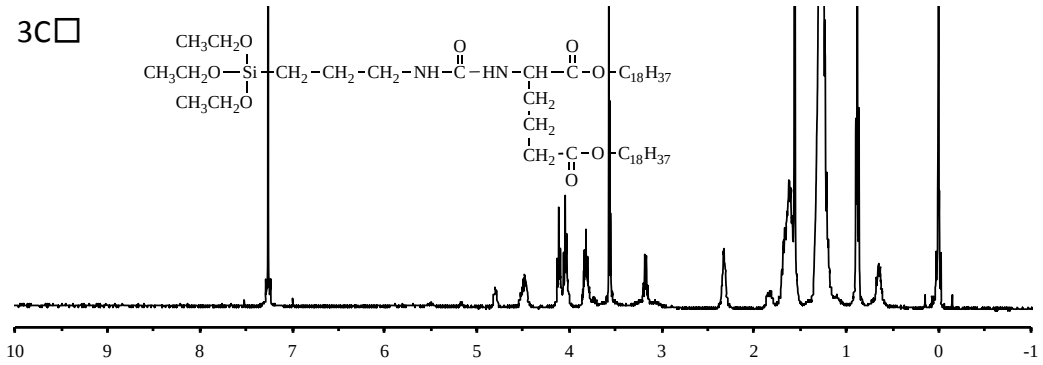

Figure S10. ^{1}H-NMR of 3c.

(TES-Asp-2C$_1$) Yield: 96.2%; Mp 51.3–51.8 °C; FT-IR (KBr, cm^{-1}): 3367 and 3331 (νN–H), 2912 and 2848 (νC–H), 1750 and 1734 (νC=O, ester), 1631 (νC=O, urea), 1572 (δN–H, urea); ^{1}H-NMR (400 MHz, $CDCl_3$): 0.62–0.66 (2H, t, $SiCH_2$) 0.88 (6H, t, CH_3), 1.26 (69H, br, CH_2 and CH_3CH_2O), 1.58–1.75 (6H, m, $COCH_2CH_2$ and $SiCH_2CH_2$), 2.80–3.03 (2H, dd, C*CH_2), 3.17–3.20 (2H, q, $NHCH_2$), 3.79–3.84 (6H, q, CH_3CH_2O), 4.05 (2H, t, OCH_2), 4.12 (2H, t, OCH_2), 4.72–4.84 (1H, m, C*H), 5.23–5.21 (1H, d, NH); Elemental analysis calcd (%) for $C_{50}H_{100}N_2O_8Si$: C 67.82, H 11.38, N 3.16; found C 67.23, H 11.94, N 3.16.

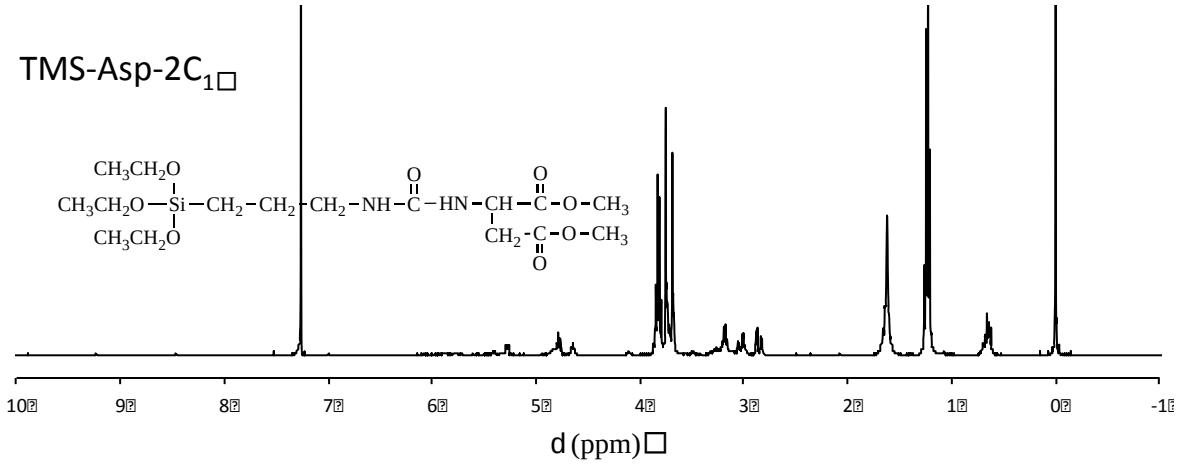

Figure S11. ^{1}H-NMR of Dimethyl ((3-(triethoxysilyl)propyl)carbamoyl)-L-aspartate (TMS-Asp-2C$_1$).

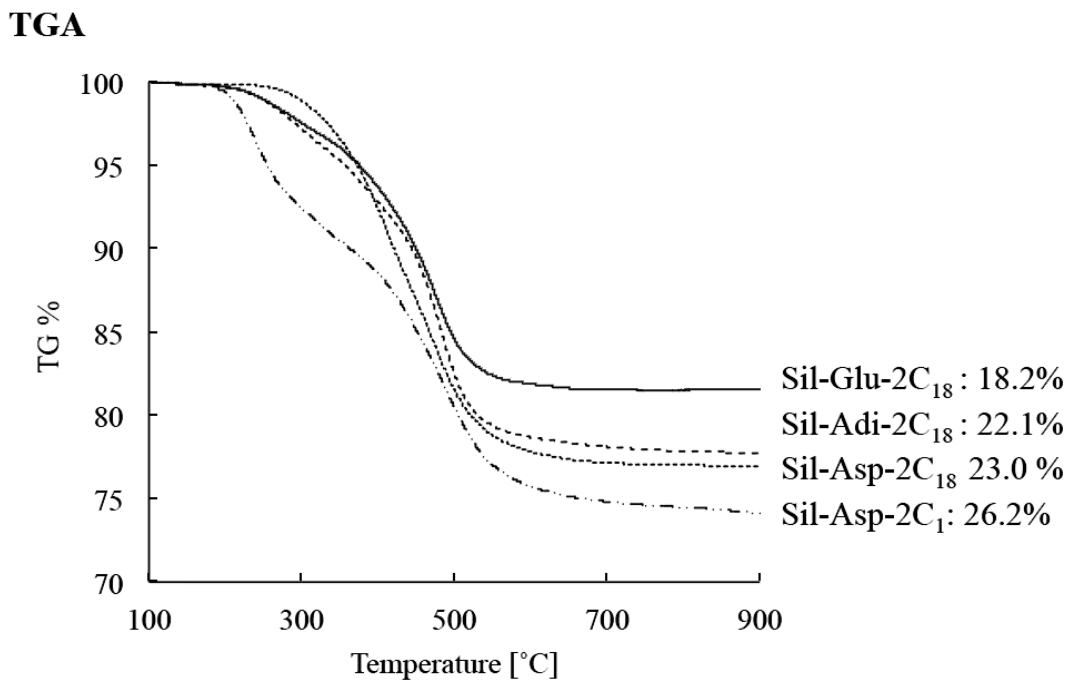

Figure S12. Thermogravimetric curves of amino acid derivatives immobilized silica.

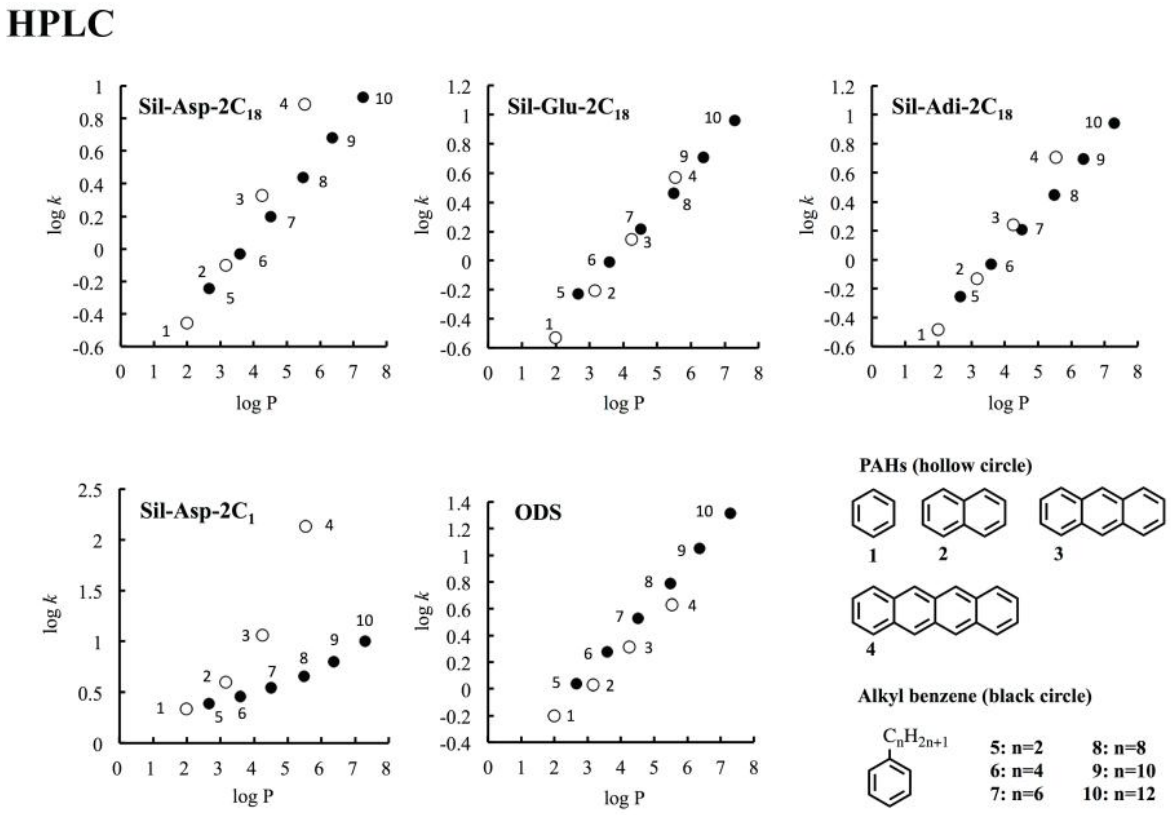

Figure S13. Relationship between the log *k* and log P of various polyaromatic hydrocarbons (PAHs) (open circle) and alkyl benzenes (filled circle) with amino acid derivatives bonded silica and octadecyl silica (ODS). Mobile phase: methanol-water (9:1), Flow rate: 1.0 mL·min^{-1}, Column temperature: 20 °C.

Table S1. Retention factors of Phenol, Resorcinol, and Phloroglucinol with Dimethyl ((3-(triethoxysilyl)propyl)carbamoyl)-L-aspartate bonded silica (Sil-Asp-2C1).

Analyte	*k*
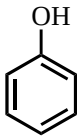 Phenol	0.11
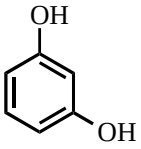 Resorcinol	0.27
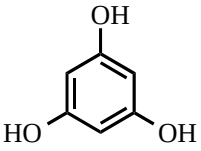 Phloroglucinol	0.52

Mobile phase: acetonitrile-10 mM ammonium acetate (9:1), flow rate: 1.0 mL·min^{-1}, Column temperature: 10 °C.

© 2016 by the authors. Submitted for possible open access publication under the terms and conditions of the Creative Commons Attribution (CC-BY) license (http://creativecommons.org/licenses/by/4.0/).